USP7 regulates melanoma progression through PI3K/Akt/FOXO and AMPK Pathways

Alexander Teichmann (✉ teichmann2020@163.com)
  The Affiliated Hospital of Southwest Medical University

Jing Jia
  The Affiliated Hospital of Southwest Medical University

Lanyang Gao
  The Affiliated Hospital of Southwest Medical University

Danli Zhu
  The Affiliated Hospital of Southwest Medical University

Qin Wang
  The Affiliated Hospital of Southwest Medical University

Shigang Yin
  The Affiliated Hospital of Southwest Medical University

Huiyan QIANG
  The Affiliated Hospital of Southwest Medical University

Heinrich Wieland
  The Affiliated Hospital of Southwest Medical University

Jinyue Zhang
  The Affiliated Hospital of Southwest Medical University

Zheng Bao
  The Affiliated Hospital of Southwest Medical University

USP7 regulates melanoma progression through PI3K/Akt/FOXO and AMPK Pathways

Lanyang Gao[2,3+], Danli Zhu[2+], Qin Wang[2+], Zheng Bao[2], Shigang Yin[3,4], Huiyan Qiang[5], Heinrich Wieland[2], Jinyue Zhang[2*], Alexander Teichmann[2*],Jing Jia[1,6*]

Lanyang Gao, Email: lanyanggao1981@163.com;Danli Zhu,Email：ZEverest@163.com; Qin Wang ,Email: wangq@swmu.edu.cn ;Zheng Bao ,Email: hitbzh@163.com ;Shigang Yin,Email:sgyin@swmu.edu.cn;Huiyan Qiang,Email ： qhy287158911@126.com;Heinrich Wieland,Email：fhwieland@163.com;Jinyue Zhang,Email:sicaujinyue@163.com;Alexander Teichmann,Email:teichmann2020@163.com;Jing Jia,Email: jiajing@swmu.edu.cn.
*Co-Corresponding author.
[+] These authors contributed equally to this work.

Abstract

Background: Increasing evidence suggests that deubiquitinase USP7 participates in tumor progression by various mechanisms and serves as a potential therapeutic target. However, its functional role in melanoma remains elusive and needs to be investigated.

Methods: The down-regulation of USP7 in A375 human melanoma cells was determined by high resolution liquid chromatography mass spectrometry (LC-MS/MS). The effects of USP7 expression on proliferation and apoptosis of melanoma cells were examined by western blot, Immunohistochemical and flow cytometry. Further study knock-down of USP7 in A375 cell lines, especially knockout USP7 using CRISPR-Cas9, verified USP7 regulate cell proliferation in vivo and in vitro .Western blot and qRT-PCR, Immunofluorescence were performed to investigate the mechanisms by which USP7 mediated melanoma growth through regulating the PI3K/Akt/FOXO pathways activity

Results: Proteomic and western blotting analysis show that inhibition of USP7 increases expression of PRKAB1, CASP7, and PPP2R3A, attenuates expression of ATP6V0C and PEX11B. Furthermore, ATP6V0C and PEX11B are proposed to be the substrate for USP7 function.

Conclusions: Our findings demonstrate that PI3K/Akt/FOXO and AMPK signaling pathways can be regulated by USP7 during melanoma progression and provide USP7 as an attractive anticancer target for melanoma.

Keywords: Melanoma,USP7, PI3K/Akt/FOXO pathways

1. Background

Malignant melanomas induced by UV radiation are the deadliest form of skin cancer that arises from melanocytes[27]. In the last five decades, the prevalence of melanoma skin cancer has been growing at an alarming rate in Caucasian populations around the world[5]. Currently, 132,000 melanoma cases occur worldwide each year (http://www.who.int/). Though melanoma is the least common form of skin cancer, it is responsible for about 80% of deaths related to cutaneous malignancies due to its metastatic potential[33]. And it is also one of the most challenging malignancies to address therapeutically. Therefore, novel targeted drugs are needed to overcome such obstacles and improve quality of life.

Ubiquitination is an enzymatic process by which proteins are modified with ubiquitin chains and this process can be reversed by deubiquitinases (DUBs). The dynamic equilibrium between ubiqutionation and deubiquitionation maintains the stability of ubiquitin-proteinase system. Aberrant DUBs activities are involved in numerous diseases, especially in tumor progression[15]. One of the few DUBs that has

been assigned a biological role is USP7, also known as Herpesvirus-associated ubiquitin-specific protease (HAUSP), which is involved in a diverse array of cellular processes. USP7 function was first identified in the context of viral infection[17]. Then, its p53-associated activities were extensively characterized[23, 24]. Several additional p53-independent functions of HAUSP were subsequently established. Accumulating evidence indicates that USP7 is involved in multiple cellular processes, including tumor progression[16, 35], immune dysfunction[37], DNA damage[21], epigenetic regulation[10], etc. Among of these processes, USP7 roles in tumor progression were extensively characterized as p53-dependent and p53-independent. Under normal conditions, USP7 perfers to associate with MDM2, a E3 ubiquitin ligase targeting p53 for degradation by the proteasome, and stabilizes MDM2, resulting in p53 turnover[24,12]. However, upon cell stress, USP7 switches from stabilizing MDM2 to p53[24]. Beyond the USP7-MDM2-p53 axis, USP7 also affects on oncogenesis through other modulators, including regulation of oncoproteins (REST, TRRAP, cMyc, etc.) [6, 18], PTEN[32], FOXO proteins[36], and Rb protein[7]. Therefore, in the past decades, researchers explored its effect on bladder[38], prostate[32], colon[4], lung[25], liver[9], ovary[42], brain[7], breast[14], glioma[11], etc. All these work demostraded that the role of USP7 is tumor suppressive or oncogenic, depending on the context of cancers and its substrates. However, the expression and role of USP7 in melanoma remains to be elucidated.

The current study is intended to investigate roles of USP7 in melanoma. We showed that USP7 was high expression in clinical melanoma tissues and its function loss significantly inhibited melanoma cells proliferation and promoted apoptosis. Mass spectrometry-based deep proteome was carried out following USP7 knockdown to explore the mechanism of action role of USP7 regulating melanoma growth. Our results showed USP7 acted as an oncogen in melanoma through mediating PI3K/AKT/FOXO as well as AMPK signaling pathways, and also through some new pathways, such as peroxisome, and lyosome signaling pathways. Concomitantly, we found ATP6V0C and PEX11B may be new substrates of USP7, which need to be confirmed furtherly. In summary, these data suggested that USP7 was a tumor promoter and can serve as a therapeutic target for melanoma, which can provide a novel therapeutic strategy to respond to the resistance of advanced melanoma to chemotherapy.

2. Materials and methods

2.1 Tissue microarray analysis

The tissue microarray (ME241b) were purchased from Alenabio (Xian, Shanxi, China), and contained 21 cases of human melanoma tissue and 4 cases of normal tissue. All specimens were performed following the protocol and ethical standard of this company. Anti-USP7 (sc-377147, Santa Cruz, 1:50) was used to immunolabel the paraffin embedded sections. USP7 expression in melanoma tissue and normal tissue were evaluated.

2.2 Immunohistochemical staining and intensity analysis

Immunohistochemistry was performed as described in literature[17]. Tumors were fixed and embedded in paraffin, followed by section. Briefly, 4 μm thick tissue sections were deparaffinized, rehydrated, and treated with antigen retrieval solution. These sections were blocked by goat serum and incubated with primary antibodie(USP7,1:50; P-Akt,1:50) then biotinylated secondary antibody(Cy3,1:100;FITC, 1:100). Finally, tissue sections were incubated with DAB and hematoxylin until color developed, then observered them by Olympus X71 fluorescence microscope. The datas were analyzed with Image J software.

2.3 Cell lines and cell culture

The A375 achromic human melanoma cell lines and Mouse B16 melanoma cell lines were cultured in Dulbecco's modified Eagle's medium (DMEM, HyClone) with high glucose (4.5 g/l) containing 100

IU/ml penicillin/streptomycin and 10% fetal bovine serum (FBS, Gibco). The 293T cells were cultured in RPMI 1640 medium (HyClone), supplemented with 100 IU/ml penicillin/ streptomycin and 10% FBS (Gibco). All the cells were cultured in 37 °C with 5% CO_2.

2.4 Transfection assay

Cells were plated in 6 cm dishes for overnight. For siRNA transfection, the complex, including 500μl RPMI opti-MEM (Gibco), siRNAS targeting USP7 and lipofectamine RNAiMax reagent (Invitrogen) was prepared to incubate with cells according to the manufacturer's instructions. After 4 hours, fresh medium was replaced. Cells were collected after incubation for 24h or 48h. The siRNA sequences were as follows: si-NC(sense 5'-UUC UCC GAA CGU GUC ACG UTT-3; antisense 5'-ACG UGA CAC GUU CGG AGA ATT-3') ; si-USP7(sense 5'-GGA CUA UGA CGU GUC UCU UTT-3'; antisense 5'-AAG AGA CAC GUC AUA GUC CTT-3').

2.5 Stable A375 USP7-ShRNA knockdown cells establishment

Sequences of shRNAs were shown as following: ShRNA-NC: 5'-CCTAAGGTTAAGTCGCCCTCG-3'; ShRNA-USP7: 5'-CGTGGTGTCAAGGTGTACTAA-3'. The sequences of USP7 ShRNA was referred to Qian Wang[40].

pCMV-dR8.2 dvpr, pLP/VSVG, and lentiviral DNA constructs (pLKO.1-TRC for USP7) were co-transfected into 293T cells using LipoFiter (HANBIO). Supernatant including lentiviruses was collected at 24 h after transfection. Lentiviruses were added to infect A375 cells overnight, and then cell lines were selected with puromycin (1 ug/ml) over 7 days.

2.6 Stable B16 CAS9-USP7 knockout cells establishment

USP7 CRISPR/Cas9 plasmid (mouse) was purchased from Santa Cruz (Santa Cruz). This plasmid was designed to disrupt gene expression by causing a double-stand break in a 5' constitutive within the USP7 (mouse) gene. The plasmid was transfected into B16 cells. After 48h transfection, B16 cells were cultured into 96 well plates at the concentration of 1 cell/well. Single colonies were picked and detected by immunoblotting analysis. USP7 knock out B16 cells and control cells were defined as B16 USP7 KO and B16 WT, respectively.

2.7 Western blot analysis

Total cell proteins were obtained from 80% confluent cell cultures. Protein extracts of whole cells were denatured, and the A375 nucleus and cytoplasm proteins were obtained by using the Nucleus and Cytoplasmic Protein Extraction Kit (Sangon Biotech) according to the manufacturer's instructions, separated by SDS–PAGE and transferred to NC membranes. After blocking with 5% skimmed milk in Tris-buffered saline-Tween, membranes were incubated with primary antibodyfor overnight at 4 °C. After incubation with the appropriate secondary antibody, results were detected using ECL detection reagent. The antibodies used were shown in table 1 as following.

2.8 Cell clonogenic assay

Clonogenic assay was performed as literature[41]. Wild type cells and USP7 loss cells (A375 shRNA-USP7 and B16 WT/USP7-KO) were plated into six well plates in triplicate for overnight. Then wild type Cells (B16 and A375) were exposed to USP7 inhibitor gen6776 (10 μm). The medium was refreshed every 3 days. The plates were washed with PBS and stained with crystal violet at the fourteenth day. The images were taken and presented.

2.9 Immunofluorescence

A375 cells were transfected with si-NC/USP7. After 24 h, cells fixed with 4% paraformaldehyde were permeabilized and blocked with 0.2% Triton X-100 and 5% FBS in PBS. Samples were then incubated with an antibody FOXO4 (1:100, Abclonal) and Ki-67 (sc-23900, 1:200, Santa Cruz) in

phosphate-buffered saline containing 0.1% Triton X-100 overnight. Incubation with the secondary FITC-labeled (Beyotime) anti-rabbit and Cy3-labeled anti-mouse antibody (Beyotime) was performed in 2.5% bovine serum albumin for 1 h at ambient temperature. The nuclei were stained with 4′,6-diamidino-2-phenylindole (DAPI) (1 μg/ml) for 5 min. Cells were visualized with a ×20 objective and a Qimaging digital camera coupled to an Olympus X71 fluorescence microscope.

2.10 Cell cycle and apoptosis assay

Cells were digested and collected. For cell cycle assay, cells were washed two times with 500 μl PBS, and added 1 ml of 70% ethanol and resuspended overnight. Then the cells were incubated with 50 μg/ml of PI, 0.2% of Triton-X-100 and 100 μg/ml of RNase complex for 30 min in dark at 4 °C. For cell apoptosis analysis, the treated cells were washed three times with PBS and centrifuged. Cells were resuspended for 30 min with a complex of 500 μl Annexin VFITC binding buffer, 5 μl PI and 5 μl Annexin V-FITC. Finally, the two samples were followed by flow cytometry.

2.11 RT-qPCR analysis

Total RNAs were extracted by TRIzol reagent (Invitrogen), and HiScript III RT SuperMix for qPCR (Vazyme) was used for reverse transcriptions according to manufacturer's instructions. The primers used for RT-qPCR were shown as following: p27^{Kip1} (forward): 5'-GGCTAACTCTGAGGACACGCA-3'; p27^{Kip1} (reverse): 5'-TGGGGAACCGTCTGAAACAT-3'; GAPDH (forward): 5'-GGAGCGAGATCCCTCCAAAAT-3'; and GAPDH (reverse): 5'-GGCTGTTGTCATACTTCTCATGG-3'. RT-qPCR was performed on LightCycler96 (Roche) using the ChamQTM SYBR qPCR Master Mix (Vazyme).

2.12 Proteomic Sample Preparation and Tandem mass tag (TMT) labeling

The siRNA transfection A375 cell samples were disrupted in SDT (4% (w/v))SDS, 100mM Tris/HCl (pH7.6, 0.1M DTT) lysis buffer. The protein concentration was determined by the BCA (Bicinchoninic acid assay) method. Then, equal amounts of protein from each group were Trypsin digestion by Filter aided proteome preparation (FASP) method and peptide concentration was determined using absorbance values at 280 nm. 100 μg of each group samples were respectively labeled using the TMT Kit (Thermo) according to the manufacturer's instructions.

2.13 High pH Reversed-Phase Peptide Fractionation and LC-MS/MS analysis

The labeled peptides in each group were mixed in equal amounts, and separated into fractions according to the High pH Reversed-Phase Peptide Fractionation Kit. Each fraction was dried, dissolved in 0.1% FA (0.1% formic acid, 5% acetonitrile), then, determined the peptide concentration at 280 nm. Each fraction sample were separated by HPLC system. The column was balanced with 95% liquid A(0.1%Aqueous formic acid), then samples flowing through the column (Thermo Scientific Acclaim PepMap100, 100 μm*2 cm, nanoViper C18) and the column (Thermo scientific EASY column, 10cm, ID75 μm, 3 μm, C18-A2) at a rate of 300 nL/min. the Q-Exactive mass spectrometer was used for detection of each fraction after separation. MS data were acquired from 300-1800 m/z for fragmentation by higher-energy collisional dissociation (HCD), with up to 20 precursors selected for LC-MS/MS and dynamic exclusion for 60s. Survey scans were acquired at a resolution of 70,000 at m/z 200 and resolution for HCD spectra was set to 17,500 at m/z 200. Full MS automatic gain control (AGC) target was 1e6, Maximum IT was 50ms and isolationwindow was 2 m/z. The normalized collision energy was 30 eV and the underfill ratio was definedas 0.1%.

2.14 Protein identification and quantitation

LC-MS/MS spectra were searched using the MASCOT engine (Matrix Science, London, UK;version

2.2) embedded into Proteome Discoverer 1.4 (Thermo Scientific). The protein ratios are calculated as the median of only unique peptides of the protein. Normalizes all peptide ratios by the median protein ratio. The median protein ratio should be 1 after the normalization.

2.15 Gene ontology and KEGG pathway enrichment analysis

To better understand the biological functions of significantly altered proteins, these proteins were analyzed using web-based GO software (http://www.geneontology.org) for gene ontology (GO) annotation and enrichment analysis. Pathway analysis was done using the web-based Kyoto Encyclopedia of Genes and Genomes (KEGG, http://www.genome.p/kegg).

2.16 Animal experiments

Nude female mice (Balb/c) and C57BL female mice were purchased from Chengdu Dossy Laboratory Animals Company and allowed to acclimatize for 1 week prior to the experiments. All animal procedures were approved by the Laboratory Animal Management Committee of the Affiliated Hospital of Southwest Medical University. Balb/c nude female mice were kept under specific pathogen-free conditions, and food, water, and bedding were autoclaved before use. All the animals used were housed in12 h light/12h dark cycle at constant temperature and provided food and water ad libitum.

Nude female mice (body weight 14-16g, 5 weeks old) were randomly divided into two group (six mice per group). Mice were inoculated subcutaneously in the right armpit with $1x10^6$ A375 shRNA-NC cells or A375 shRNA-USP7 cells in 100 µl PBS to induce the tumor. Weight and tumor size of mice were measured at day 6 post tumor transplantation and every three days. Tumor volume was calculated according to the formula $V=0.5 \times a^2 \times b$ (a, smallest superficial diameter; b, largest superficial diameter). The mice were killed by CO_2 overdose at day 29 post treatments. The tumors were harvested, weighted, and recorded.

C57BL female mice (body weight 13-15g, 5 weeks old) were also randomly divided into two group (six mice per group). B16 WT melonoma cells or B16 USP7-KO melonoma cells were subcutaneously injected into their right armpit with the viable cell number $3x10^5$ cells. Weight and tumor size of mice were measured at day 6 post tumor transplantation and every three days. The mice were killed by CO_2 overdose at day 15 post treatments. The tumors were analyzed..

2.17 Statistical analysis

Statistical analysis was performed with GraphPad Prism software. The data shown in the figures were representative of three or more independent experiments and were analyzed by one way Student's t-test, and $P < 0.05$ was considered statistically significant. Where exact P-values are not shown, statistical significance is shown as with *$P < 0.05$, **$P < 0.01$, and ***$P < 0.001$.

3. Results

3.1 USP7 is overexpressed in melanoma and predicts clinical outcome

To date, early studies have demonstrated that USP7 plays a prominent role in tumor development and progression[7, 9, 32]. To identify the role of USP7 in melanoma, we analyzed the expression levels of USP7 in human normal skin and melanoma by immunohistochemistry assay. We found that the expression of this protein was increased in human melanoma tissues compared with normal skin tissue (Fig. 1a, b). To further examine the clinical importance of USP7 in melanoma patients, we performed Kaplan–Meier analysis in melanoma patients of TCGA. Our results showed that USP7 expression was negatively correlated with overall survival of melonoma patients in TCGA dataset (P<0.05, Fig. 1c). Collectively, these results demonstrate that USP7 is overexpressed in human melanoma and predicts clinical outcome.

3.2 USP7 loss suppresses melanoma growth

To explore the USP7 expression relative to the melanoma development and progression, we built USP7 knockdown A375 cells by short hairpin RNA (shRNA) or siRNA and USP7 KO B16 cells as we described in material and methods (Fig. 2a). The cell colony formation assay results revealed that USP7 function loss dramatically suppressed the colony formation (Fig. 2b). Furthermore, Fig. 2c-e showed that PARP cleavage and cellular apoptosis were induced by USP7 inhibition. The cell apoptosis rate increased from 2% of control to 6.97% of treatment cells. Concomitantly, the USP7 downregulation significantly arrested the cell cycle, increasing the proportion of A375 cells in the G1 phase and decreasing the proportion in the S-phase (Fig. 2g, h). And the proliferation maker Ki67 expression was also reduced by USP7 downregulation (Fig. 2f). These findings supported a role of USP7 in promoting growth of melanoma cells.

3.3 Protein identification and quantification

To clarify the mechanism of action role of USP7 in melanoma, we compared whole-cell proteomes before and 24h after knockdown of USP7 in A375 cells using TMT quantitative proteomics technology. As a result, we identified a total of 5696 proteins with expression multiple changes of 1.1 times or more (upregulation greater than 1.1 times or down-regulation less than 0.909 times) and P value<0.05. In si-USP7 vs si-NC group, we found 101 up-regulated differentially expressed proteins (DEPs) and 71 down-regulated differentially expressed proteins (Supplement1, a). Supplement 1, b shows a hierarchical clustering analysis of all 172 DEPs.

3.4 Bioinformatics Analysis

To obtain a biological view of the identified proteins, we carried out the GO analysis using Blast2GO sofeware. A total of 5696 proteins were annotated by molecular function, biological process and cellular components. Then, fisher accurate test was used to analyze the GO function enrichment of the differentially expressed proteins. The top 10 enriched GO terms within each major functional category were shown in Fig. 3a and Supplement 1c. In three categories, the most significant terms are all associated with microtubule-related functions (microtubule-based movement, microtubule motor activity and kinesin complex). These microtubule-related terms are all involved in the DEPS of KIF20A, KIF20B, KIF13B and KIF1B. These kinesins in protein-protein interaction network form a cluster with microtubule motor activity (Fig. 3b). Multiple studies have shown that knockdown of KIF20B in bladder, liver and HCT116 colon cancer cells results in cytokinetic defects that are reflected in accumulation of multinucleated cells that eventually undergo apoptosis

It is well known that these proteins mediate cytokinesis and microtubule movement and transport due to their protein kinase binding, ATPase activity and microtubule motor activity, which indicates that the potential of USP7 to regulate melanoma cells growth may be in connection with microtubule associated activity.

Moreover, in the biological process and molecular function category, we noted that many terms are related to nucleoside-containing compound biosynthetic and metabolic, for instance, CTP metabolic process, pyrimidine ribonucleoside triphosphate biosynthetic process, nucleobase-containing compound kinase activity and so on (Fig. 3a). The nucleoside kinases of NME1, NME2P1, UCK2 and UCK1, within in these terms, were significantly upregulated as USP7 downregulation, indicating that USP7 impacted on the nucleotides-metabolism-associated protome. Additionally, one of these, NME1, was reported as a metastasis suppressor according previous studies[34], which provided a clue to explain how USP7 influence on metastasis of melanoma.

In addition to the functional categories mentioned above, a range of others were identified in DEPS in

response to USP7 knockdown, including ferric iron binding, transition metal ion transmembrane transporter activity and zinc ion transmembrane transporter activity. To explore these functional categories, we identified protein-protein interaction networks significantly altered in the protein sets, as shown in Figure 3b. Among proteins involved in ion transport and binding (Fig. 3b-3, 4), ATP6V0C is top1 decreased protein following USP7 knockdown, which was also confirmed by western blotting (Fig. 4a). Previous studies have reported that ATP6V0C was high expression in metastatic prostate cancer and its silence effectively suppressed the migration and invasion of prostate carcinoma cells[43]. Therefore, USP7 downregulation likely inhibited the migration and invasion of melanoma through regulating ATP6V0C expression.

Protein-protein interaction networks then revealed another four distinct clusters (Fig. 3b), corresponding to proteins related to DNA repair, post-translational protein modification, microtubule motor activity, and ubiquitin-protein transferase activity. The significantly decreased DEPS from Cluster 1 are RNF169, MLLT1 and NCOA6, which are all associated with DNA repair. This seems to confirm the DNA damage repair function of USP7. Moreover, early works on USP7 showed that USP7 deubiquitylates and stabilizes RNF169 in response to DNA double-strand breaks[2]. This suggests that USP7 in melanoma may have the same effect on RNF169 in response to DNA damage.

As for cluster 5, it mainly consists of kinesin and dynein, which are associated with cells proliferation, apoptosis inhibition and carcinogenic progression[19]. In cluster 2 and 6, molecular functions or biological processes of proteins are related post-translational protein modification and ubiquitin-protein transferase activity. Many E3 ubiquitin ligases use USP7 DUB activity to prevent autoubiquitination[22]. Consequently, we inferred that USP7 regulated melanoma cells growth through modifying the stability of multiple proteins.

Overall, GO and protein-protein interaction analyses provide a certain understanding the DEPS in biological process and molecular function. To explore how USP7 plays roles in melanoma by these cellar processes, DEPS were then mapped to the reference pathway in the KEGG database. 172 DEPS were mapped to 178 signaling pathways. PIK3CB is the most protein participating in signaling pathways, followed by PRKAB1, CASP7, PPP2R3A and ATP6V0C. we confirmed these proteins in both A375 and B16 cell lines (Fig.4a). These results indicate that the roles of USP7 through these four proteins are conserved in different types of melanoma cells. In addition, the pathways containing upregulated or downregulated top5 proteins may also be the crucial role of USP7 in melanoma, such as ATP6V0C and PEX11B. Therefore, the pathways involving in PRKAB1, CASP7, PPP2R3A, ATP6V0C and PEX11B were selected for further study. Concomitantly, only the pathways with at least three or more DEPs are shown in Fig. 3c. In present study, we mainly focus on PI3K-Akt, FOXO and AMPK signaling pathways to clarify the roles of USP7 in melanoma.

3.5 **Validation of proteomic data**

To validate our mass spectrometry results, we obtained antibodies against a subset of the identified proteins and analyzed their expression levels after removal of USP7 by Western blotting. We confirmed the two most striking DEPS of ATP6V0C and PEX11B (Fig. 4a). Next, PRKAB1 (AMPK), CASP7 and PPP2R3A, which participate in many pathways, were also confirmed (Fig. 4a). Altogether, the proteins of ATP6V0C, PRKAB1, CASP7, PPP2R3A, and PEX11B were confirmed in both melanoma cell lines after USP7 loss, which indicated that USP7 may control the signaling pathways involving in these proteins to promote melanoma development and progression. For example, Kaplan–Meier analysis of ATP6V0C and CASP7 in melanoma patients of TCGA showed that the two proteins expression were negatively and positively correlated with overall survival of melonoma patients

(P<0.05 for ATP6V0C and P<0.05 for CASP7, supplement 2), respectively. Moreover, ATP6V0C and PEX11B, dramatically decreased protein as USP7 function loss, were proposed to be the substrate for USP7 function.

3.6 Reduction of USP7 mediates signaling pawthways associated with cancer activity

PPP2R3A and PRKAB1 were authenticated by immunoblotting analysis after USP7 removal in two melanoma cell lines. It is well-known that the two proteins play crucial roles in PI3K/AKT/FOXO and AMPK signaling pathways, respectively. To determine whether these proteins indeed play roles in the two pathways, we detected the phosphorylation levels of key proteins of signaling pathway using immunoblotting assay. Our result showed that phosphorylated AMPK is significantly increased following USP7 loss in both cell lines A375 and B16 (Fig. 4b), which may be due to the PRKAB1 increasing. Previous studies have proposed a tumor-suppressing function of activated AMPK[29, 30]. Accordingly, USP7 loss inhibits melanoma growth by activating AMPK signaling pathway partially.

In agreement with previous work with USP7 [8, 32, 36], our results also suggested that USP7 can activate PI3K/Akt signaling pathway to promote cell survival by phosphorylating and inhibit forkhead box O transcription factors (FOXO), such as FOXO1, FOXO3a and FOXO4. As shown in (Fig. 4a and b), phosphorylated Akt decreases due to the increasement of PPP2R3A which can dephosphorylate Akt. These results indicated that USP7 as an oncogene positively controlled cell growth and inhibited cell apoptosis through activiting PI3K/Akt signaling pathway in melanoma. Further research found that Akt phosphorylation reduction resulted in FOXO dephosphorylation at Akt-induced sites, including P-FOXO4(Thr28), P-FOXO3a(Thr32), P-FOXO1(Thr24) (Fig. 4b). According pervious studies[8], we know that decrease of FOXO phosphorylation promotes them to entry into the nucleus and ultimately increases transcriptional activity towards target genes, including the cell cycle arrest gene p27^{kip1}. To further confirm this result in melanoma, FOXO4 were selected for detecting its intracellular localization by immunofluorescence and nuclear/cytosol protein fractionation assay and its target gene p27^{kip1} expression level. Result showed that FOXO4 was mainly present in the nuclear compartment after USP7 downregulation (Fig. 4c, d), which ultimately promoted gene p27^{kip1} expression (Fig. 4e). Armando[36] has reported that USP7 deubiquitylates FOXO4, resulting in a nuclear exclusion, and inhibiting FOXO4 transcription activity. Therefore, USP7 deubiquitination may also contribute to FOXO4 accumulation in nucleus.

In all, our results suggested that USP7 function loss inhibited melanoma cell cycle and promoted cell apoptosis by mediating AMPK and PI3K/Akt/FOXO signaling pathways activity in part.

3.7 USP7 loss suppresses melanoma growth in A375 and B16 xenografts

To confirm the role of USP7 in melanoma *in vivo*, shRNA-USP7 A375 cells and USP7-KO B16 cells xenograft models were established in Balb/c nude mice and C57BL mice, respectively. As shown in Fig. 5(a,b,c), there was a significant reduction in tumor growth and tumor weight after USP7 loss, with tumor volumes inhibited by 64.7% for A375 and 46.4% for B16. While the body weight between control and USP7 loss group, no significant change was observed.

To further validate the mechanism of action role of USP7 as an oncogen in melanoma *in vivo*, the expression levels of indicated proteins in Fig. 5 were analyzed by immunoblotting and immunohistochemistry. Fig. 5e and f show that in line with proteomic results, the indicated proteins and have significant changes on levels in both A375 and B16 cells after USP7 loss. These findings further supported that USP7 mediated melanoma growth through regulating the proteins of ATP6V0C, PRKAB1, CASP7, PPP2R3A, and PEX11B expression and AMPK and PI3K/Akt/FOXO pathways activity.

4. Discussion

HAUSP/USP7 has attracted attention due to its capacity to interact with the viral proteins EBNA-1 and ICP0, and because it affects the stability of p53 and MDM2 [28, 31], placing it at the heart of the biological function of key regulatory molecules. Therefore, the multi-dimensional role of USP7 is established in various cancers, including prostate cancer, lung cancer, brain cancer, colon cancer, breast cancer, epithelial ovarian carcinoma (EOC), liver cancer, and leukemia. These data support several context-specific tumor suppressive and oncogenic outcomes. High levels of USP7 are directly correlated with tumor aggressiveness in human prostate cancer[32]. Conversely, Masuya found that a reduction in USP7 gene expression may play an important role in non-small cell lung cancer (NSCLC)[25]. However, the roles of USP7 in melanoma are unclear until now.

We found that USP7 levels were higher in melanoma than that in normal skin and were associated with poorer prognosis based on the analysis from TCGA datasets. These findings implied that USP7 implicated in melanoma development and progression. Next, studies in A375 and B16 cells demonstrated that USP7 function loss inhibited cell growth through promoting cell cycle arrest and apoptosis. Furthermore, we explored the mechanism of action role of USP7 regulating melanoma growth by detecting proteomic profiling following USP7 knockdown in A375 cells. Proteomic data analysis and western blot results showed that classical signaling pathways PI3K/Akt/FOXO and AMPK, and new biological processes involved proteins such as ATP6V0C, CASP7, and PEX11B played crucial roles in USP7 mediating melanoma growth. USP7 knockdown decreased the Akt phosphorylation and then caused FOXO phosphorylation reduction, which ultimately increased FOXO accumulation in nucleus and promoted P27^{kip1} gene expression that arrested cell cycle (Fig. 4).

According our results and previous studies with USP7, we know that there are two aspects of Akt phosphorylation reduction have to be addressed. The first reason involves that PPP2R3A, a regulatory subunits of the protein phosphatase 2 (PP2A), significantly increased after USP7 downregulation. A previous study has shown that PP2A can directly dephosphorylate Akt, inhibiting PI3K/Akt singnaling pawthway activity[39]. The second reason relates to the intracellular localization of PTEN which antagonizes the PI3K-AKT pathway. Previous reports demonstrate that USP7 induces PTEN deubiquitination, causing PTEN's exclusion from the nucleus and subsequently increase in PI3K/AKT signaling pathway[3]. Therefore, USP7 downregulation accumulates monoubiquitinated PTEN in nucleus, reducing Akt phosphorylation. Collectively, the two aspects explain how USP7 plays a role in melanoma through PI3K-AKT pathway.

Further research showed Akt phosphorylation reduction induced FOXO dephosphorylation at Akt-induced sites. It is reported that phosphorylated FOXO induced by activated Akt stays in cytosol and is imported to the nucleus through dephosphorylation to induce the expression of a series of target proteins that regulate metabolism, the cell cycle, and apoptosis[26]. Our results show that phosphorylations of FOXO4 (Thr28), FOXO3a (Thr32) and FOXO1 (Thr24) significantly decrease and FOXO4 remarkably accumulates in nucleus following USP7 knockdown. Of course, FOXO4 accumulation in nucleus may be caused by weaking deubiquitination of USP7 downregulation. Similar as PTEN, USP7-induced FOXO4 deubiquitination results in nuclear export and eliminates its transcriptional activity[36]. Even so, we can not deny that a dephosphorylated FOXO caused by Akt phosphorylation reduction promotes FOXO accumulation in nucleus, inducing the expression of proteins related to the cell cycle, and apoptosis. Consequently, we can draw a conclusion that USP7 controls melanoma cells proliferation and apoptosis via regulating PI3K/Akt/FOXO4 signaling pathway in part.

KEGG analysis of proteomic data and western blot results exhibit that AMPK singnaling pathway also plays a role in USP7 mediating melanoma growth. PRKAB1, a regulatory subunit of the AMP-activated protein kinase (AMPK), has a remarkable increment following USP7 function loss, which ultimately raises AMPK phosphorylation and activates AMPK signaling. It is well-documented that AMPK signaling has anti-proliferative role. Dai and her colleagues have reported that activated AMPK signaling inhibits survival and proliferation and activates apoptosis in colorectal cancer cells[13]. Consequently, USP7 also plays a role in melanoma through AMPK signaling.

USP7 as a context-specific modulator mediates p53-dependent apoptosis via controlling MDM2 stability. And inhibition of USP7 also induce endoplasmic reticulum (ER) stress due to accumulation of polyubiquitinated protein substrates in cancer cells, which leads to increased intracellular reactive oxygen species (ROS). Increased ROS are able to cause apoptosis in these cells. Our results indicate that USP7 knockdown also induce apoptosis (Fig. 2). A lack of USP7-dependent deubiquitylation of mdm2 may lead, through enhanced breakdown of mdm2, to accumulation of p53 in melanoma. However, our data suggests additional involvement of USP7 in alternative apoptotic pathways, possibly via modification of caspase7 dependent mechanism. In line with these observations, we found cleaved PARP1 levels increased upon USP7 removal. Similarly, in colon carcinoma cells USP7 is involved in apoptotic pathways by modifying caspase3 level[20]. Therefore, we confirm that USP7 also as a oncogen inhibit p53-dependent apoptosis in melanoma like as in colon cancer.

Proteins regulated by USP7 of ATP6V0C and PEX11B are confirmed in both melanoma cell lines by western blot assay. It is reported that and ATP6V0C is involved in the migration and invasion of prostate carcinoma cells[43]. In addition, enriched KEGG pathways show that ATP6V0c and PEX11B are key protein of lysosome and peroxisome, respectively. These findings provide a cue that USP7 plays new roles in melanoma through these two pathways which have not been reported in other cancers.

Previous results demonstrated that inhibition of USP7 induced genotoxic stress and DNA damage in CLL cells[1]. We also got similar results in melanoma cells following USP7 knockdown. GO analysis suggests that DEPS of RNF169, XPA, MLLT1 and NCOA6 participate in DNA repair (Fig. 3). One of these, E3 ubiquitin ligases RNF169 deubiquitylated and stabilized by USP7 in response to DNA double-strand breaks[2], significantly decreased as USP7 knockdown, which suggests USP7 in melanoma also play a role in DNA repair.

5.Conclusion

our study built the first proteome in A375 cells following USP7 knockdown and regarded the role of USP7 protein in melanoma proliferation and apoptosis. Our results demonstrated that USP7 as an oncogene like in colorectal cancer and prostate cancer regulates melanoma development and progression through PI3K/AKT/FOXO4 and AMPK signaling pathway and also some new pathways, such as lysosome, peroxisome. With follow-up validation, proteins such as ATP6V0c that was significantly downregulated as USP7 knockdown may be as new USP7's substrates. Thus, these findings suggest that USP7 represents a promising therapeutic target in melanoma.

Abbreviations

CRISPR: Clustered regularly interspaced short palindromic repeats; qRT-PCR: Quantitative reverse transcription polymerase chain reaction.

Ethics approval and consent to participate

All animal procedures were approved by the Laboratory Animal Management Committee of the Affiliated Hospital of Southwest Medical University. All animal experiments were performed under ARRIVE (Animal Research: Reporting of in vivo Experiments) guidelines

Consent for publication

Not applicable.

Availability of supporting data

Not applicable.

Competing interests

The authors declare that they have no competing interests

Authors' contributions

JJ and AT designed the study. LYG and JYZ drafted the manuscript. DLZ, JJ and LYG conducted experiments, and the other authors took part in literature collection and data analysis as assistants. All authors read and approved the final manuscript.

Author details

1 Department of Anesthesiology, The Affiliated Hospital of Southwest Medical University, Luzhou, Sichuan , 646000, China

2 Sichuan Provincial Center for Gynaecology and Breast Disease, The Affiliated Hospital of Southwest Medical University, Luzhou, Sichuan , 646000, China

3 Academician (Expert)Workstation of Sichuan Province, Affiliated hospital of southwest medical university, Luzhou,646000, China

4 Laboratory of Nervous System Disease and Brain Functions, the Affiliated Hospital of Southwest Medical University, Luzhou, 646000, China

5 Department of outpatient, the Affiliated hospital of southwest medical university, Luzhou, 646000, China

6 Laboratory of Anesthesiology, Southwest Medical University, Luzhou, 646000, China

References

1   A. Agathanggelou, E. Smith, N. J. Davies, M. Kwok, A. Zlatanou, C. E. Oldreive, J. Mao, D. Da Costa, S. Yadollahi, T. Perry, P. Kearns, A. Skowronska, E. Yates, H. Parry, P. Hillmen, C. Reverdy, R. Delansorne, S. Paneesha, G. Pratt, P. Moss, A. M. R. Taylor, G. S. Stewart, and T. Stankovic, 'Usp7 Inhibition Alters Homologous Recombination Repair and Targets Cll Cells Independently of Atm/P53 Functional Status', *Blood,* 130 (2017), 156-66.

2   L. An, Y. Jiang, H. H. Ng, E. P. Man, J. Chen, U. S. Khoo, Q. Gong, and M. S. Huen, 'Dual-Utility Nls Drives Rnf169-Dependent DNA Damage Responses', *Proc Natl Acad Sci U S A,* 114 (2017), E2872-E81.

3   J. T. Barata, 'The Impact of Pten Regulation by Ck2 on Pi3k-Dependent Signaling and Leukemia Cell Survival', *Adv Enzyme Regul,* 51 (2011), 37-49.

4   K. Becker, N. D. Marchenko, G. Palacios, and U. M. Moll, 'A Role of Hausp in Tumor Suppression in a Human Colon Carcinoma Xenograft Model', *Cell Cycle,* 7 (2008), 1205-13.

5   F. Belanger, V. Rajotte, and E. A. Drobetsky, 'A Majority of Human Melanoma Cell Lines Exhibits an S Phase-Specific Defect in Excision of Uv-Induced DNA Photoproducts', *PLoS One,* 9 (2014), e85294.

6   S. Bhattacharya, and M. K. Ghosh, 'Hausp Regulates C-Myc Expression Via De-Ubiquitination of Trrap', *Cell Oncol (Dordr),* 38 (2015), 265-77.

7   ———, 'Hausp, a Novel Deubiquitinase for Rb - Mdm2 the Critical Regulator', *FEBS J,* 281 (2014), 3061-78.

8   A. Brunet, A. Bonni, M. J. Zigmond, M. Z. Lin, P. Juo, L. S. Hu, M. J. Anderson, K. C. Arden, J. Blenis, and M. E. Greenberg, 'Akt Promotes Cell Survival by Phosphorylating and Inhibiting a Forkhead Transcription Factor', *Cell,* 96 (1999), 857-68.

9   J. B. Cai, G. M. Shi, Z. R. Dong, A. W. Ke, H. H. Ma, Q. Gao, Z. Z. Shen, X. Y. Huang, H. Chen, D. D. Yu, L. X. Liu, P. F. Zhang, C. Zhang, M. Y. Hu, L. X. Yang, Y. H. Shi, X. Y. Wang, Z. B. Ding, S. J. Qiu, H. C. Sun, J. Zhou, Y. G. Shi, and J. Fan, 'Ubiquitin-Specific Protease 7 Accelerates P14(Arf) Degradation by Deubiquitinating Thyroid Hormone Receptor-Interacting Protein 12 and Promotes Hepatocellular Carcinoma Progression', *Hepatology,* 61 (2015), 1603-14.

10   D. Chauhan, Z. Tian, B. Nicholson, K. G. Kumar, B. Zhou, R. Carrasco, J. L. McDermott, C. A. Leach, M. Fulcinniti, M. P. Kodrasov, J. Weinstock, W. D. Kingsbury, T. Hideshima, P. K. Shah, S. Minvielle, M. Altun, B. M. Kessler, R. Orlowski, P. Richardson, N. Munshi, and K. C. Anderson, 'A Small Molecule Inhibitor of Ubiquitin-Specific Protease-7 Induces Apoptosis in Multiple Myeloma Cells and Overcomes Bortezomib Resistance', *Cancer Cell,* 22 (2012), 345-58.

11   C. Cheng, C. Niu, Y. Yang, Y. Wang, and M. Lu, 'Expression of Hausp in Gliomas Correlates with Disease Progression and Survival of Patients', *Oncol Rep,* 29 (2013), 1730-6.

12   J. M. Cummins, C. Rago, M. Kohli, K. W. Kinzler, C. Lengauer, and B. Vogelstein, 'Tumour Suppression: Disruption of Hausp Gene Stabilizes P53', *Nature,* 428 (2004), 1 p following 486.

13   C. Dai, X. Zhang, D. Xie, P. Tang, C. Li, Y. Zuo, B. Jiang, and C. Xue, 'Targeting Pp2a Activates Ampk Signaling to Inhibit Colorectal Cancer Cells', *Oncotarget,* 8 (2017), 95810-23.

14   M. T. Epping, L. A. Meijer, O. Krijgsman, J. L. Bos, P. P. Pandolfi, and R. Bernards, 'Tspyl5 Suppresses P53 Levels and Function by Physical Interaction with Usp7', *Nat Cell Biol,* 13 (2011), 102-8.

15   J. Heideker, and I. E. Wertz, 'Dubs, the Regulation of Cell Identity and Disease', *Biochem J,* 465 (2015), 1-26.

16   S. Hernandez-Perez, E. Cabrera, E. Salido, M. Lim, L. Reid, S. R. Lakhani, K. K. Khanna, J. M. Saunus, and R. Freire, 'Dub3 and Usp7 De-Ubiquitinating Enzymes Control Replication Inhibitor Geminin: Molecular Characterization and Associations with Breast Cancer', *Oncogene,* 36 (2017), 4817.

17   H. Huang, M. Guo, N. Liu, C. Zhao, H. Chen, X. Wang, S. Liao, P. Zhou, Y. Liao, X. Chen, X. Lan, J. Chen, D. Xu, X. Li, L. Shi, L. Yu, Y. Nie, X. Wang, C. E. Zhang, and J. Liu, 'Bilirubin Neurotoxicity Is Associated with Proteasome Inhibition', *Cell Death Dis,* 8 (2017), e2877.

18   Z. Huang, Q. Wu, O. A. Guryanova, L. Cheng, W. Shou, J. N. Rich, and S. Bao, 'Deubiquitylase Hausp Stabilizes Rest and Promotes Maintenance of Neural Progenitor Cells', *Nat Cell Biol,* 13 (2011), 142-52.

19   M. Kanehira, T. Katagiri, A. Shimo, R. Takata, T. Shuin, T. Miki, T. Fujioka, and Y. Nakamura, 'Oncogenic Role of Mphosph1, a Cancer-Testis Antigen Specific to Human Bladder Cancer', *Cancer Res,* 67 (2007), 3276-85.

20   B. M. Kessler, E. Fortunati, M. Melis, C. E. Pals, H. Clevers, and M. M. Maurice, 'Proteome Changes Induced by Knock-Down of the Deubiquitylating Enzyme Hausp/Usp7', *J Proteome Res,* 6 (2007),

4163-72.

21 H. Kim, J. M. Lee, G. Lee, J. Bhin, S. K. Oh, K. Kim, K. E. Pyo, J. S. Lee, H. Y. Yim, K. I. Kim, D. Hwang, J. Chung, and S. H. Baek, 'DNA Damage-Induced Roralpha Is Crucial for P53 Stabilization and Increased Apoptosis', *Mol Cell,* 44 (2011), 797-810.

22 R. Q. Kim, and T. K. Sixma, 'Regulation of Usp7: A High Incidence of E3 Complexes', *J Mol Biol,* 429 (2017), 3395-408.

23 M. Li, C. L. Brooks, N. Kon, and W. Gu, 'A Dynamic Role of Hausp in the P53-Mdm2 Pathway', *Mol Cell,* 13 (2004), 879-86.

24 M. Li, D. Chen, A. Shiloh, J. Luo, A. Y. Nikolaev, J. Qin, and W. Gu, 'Deubiquitination of P53 by Hausp Is an Important Pathway for P53 Stabilization', *Nature,* 416 (2002), 648-53.

25 D. Masuya, C. Huang, D. Liu, T. Nakashima, H. Yokomise, M. Ueno, N. Nakashima, and S. Sumitomo, 'The Hausp Gene Plays an Important Role in Non-Small Cell Lung Carcinogenesis through P53-Dependent Pathways', *J Pathol,* 208 (2006), 724-32.

26 H. Matsuzaki, A. Ichino, T. Hayashi, T. Yamamoto, and U. Kikkawa, 'Regulation of Intracellular Localization and Transcriptional Activity of Foxo4 by Protein Kinase B through Phosphorylation at the Motif Sites Conserved among the Foxo Family', *J Biochem,* 138 (2005), 485-91.

27 Ana Catarina Menezes, Sara Raposo, Sandra Simões, Helena Ribeiro, Helena Oliveira, and Andreia Ascenso, 'Prevention of Photocarcinogenesis by Agonists of 5-Ht1a and Antagonists of 5-Ht2a Receptors', *Molecular neurobiology,* 53 (2016), 1145-64.

28 J. Parkinson, and R. D. Everett, 'Alphaherpesvirus Proteins Related to Herpes Simplex Virus Type 1 Icp0 Affect Cellular Structures and Proteins', *J Virol,* 74 (2000), 10006-17.

29 C. T. Pineda, and P. R. Potts, 'Oncogenic Magea-Trim28 Ubiquitin Ligase Downregulates Autophagy by Ubiquitinating and Degrading Ampk in Cancer', *Autophagy,* 11 (2015), 844-6.

30 R. L. Plews, A. Mohd Yusof, C. Wang, M. Saji, X. Zhang, C. S. Chen, M. D. Ringel, and J. E. Phay, 'A Novel Dual Ampk Activator/Mtor Inhibitor Inhibits Thyroid Cancer Cell Growth', *J Clin Endocrinol Metab,* 100 (2015), E748-56.

31 Z. Ronai, 'Balancing Mdm2 - a Daxx-Hausp Matter', *Nat Cell Biol,* 8 (2006), 790-1.

32 M. S. Song, L. Salmena, A. Carracedo, A. Egia, F. Lo-Coco, J. Teruya-Feldstein, and P. P. Pandolfi, 'The Deubiquitinylation and Localization of Pten Are Regulated by a Hausp-Pml Network', *Nature,* 455 (2008), 813-7.

33 L. R. Strickland, H. C. Pal, C. A. Elmets, and F. Afaq, 'Targeting Drivers of Melanoma with Synthetic Small Molecules and Phytochemicals', *Cancer Lett,* 359 (2015), 20-35.

34 C. Y. Tan, and C. L. Chang, 'Ndpka Is Not Just a Metastasis Suppressor - Be Aware of Its Metastasis-Promoting Role in Neuroblastoma', *Lab Invest,* 98 (2018), 219-27.

35 O. Tavana, D. Li, C. Dai, G. Lopez, D. Banerjee, N. Kon, C. Chen, A. Califano, D. J. Yamashiro, H. Sun, and W. Gu, 'Hausp Deubiquitinates and Stabilizes N-Myc in Neuroblastoma', *Nat Med,* 22 (2016), 1180-86.

36 A. van der Horst, A. M. de Vries-Smits, A. B. Brenkman, M. H. van Triest, N. van den Broek, F. Colland, M. M. Maurice, and B. M. Burgering, 'Foxo4 Transcriptional Activity Is Regulated by Monoubiquitination and Usp7/Hausp', *Nat Cell Biol,* 8 (2006), 1064-73.

37 J. van Loosdregt, V. Fleskens, J. Fu, A. B. Brenkman, C. P. Bekker, C. E. Pals, J. Meerding, C. R. Berkers, J. Barbi, A. Grone, A. J. Sijts, M. M. Maurice, E. Kalkhoven, B. J. Prakken, H. Ovaa, F. Pan, D. M. Zaiss, and P. J. Coffer, 'Stabilization of the Transcription Factor Foxp3 by the Deubiquitinase Usp7 Increases Treg-Cell-Suppressive Capacity', *Immunity,* 39 (2013), 259-71.

38   N. Varol, E. Konac, and C. Y. Bilen, 'Does Wnt/Beta-Catenin Pathway Contribute to the Stability of Dnmt1 Expression in Urological Cancer Cell Lines?', *Exp Biol Med (Maywood),* 240 (2015), 624-30.

39   E. Wandzioch, M. Pusey, A. Werda, S. Bail, A. Bhaskar, M. Nestor, J. J. Yang, and L. M. Rice, 'Pme-1 Modulates Protein Phosphatase 2a Activity to Promote the Malignant Phenotype of Endometrial Cancer Cells', *Cancer Res,* 74 (2014), 4295-305.

40   Q. Wang, S. Ma, N. Song, X. Li, L. Liu, S. Yang, X. Ding, L. Shan, X. Zhou, D. Su, Y. Wang, Q. Zhang, X. Liu, N. Yu, K. Zhang, Y. Shang, Z. Yao, and L. Shi, 'Stabilization of Histone Demethylase Phf8 by Usp7 Promotes Breast Carcinogenesis', *J Clin Invest,* 126 (2016), 2205-20.

41   X. Xia, Y. Liao, C. Huang, Y. Liu, J. He, Z. Shao, L. Jiang, Q. P. Dou, J. Liu, and H. Huang, 'Deubiquitination and Stabilization of Estrogen Receptor Alpha by Ubiquitin-Specific Protease 7 Promotes Breast Tumorigenesis', *Cancer Lett,* 465 (2019), 118-28.

42   L. Zhang, H. Wang, L. Tian, and H. Li, 'Expression of Usp7 and March7 Is Correlated with Poor Prognosis in Epithelial Ovarian Cancer', *Tohoku J Exp Med,* 239 (2016), 165-75.

43   P. Zou, Y. Yang, X. Xu, B. Liu, F. Mei, J. You, Q. Liu, and F. Pei, 'Silencing of Vacuolar Atpase C Subunit Atp6v0c Inhibits the Invasion of Prostate Cancer Cells through a Lass2/Tmsg1-Independent Manner', *Oncol Rep,* 39 (2018), 298-306.

Figure legends

Fig. 1 USP7 is overexpressed in melanoma and predicts clinical outcome. (a,b) Immunohistochemical analysis of USP7 in human normal skin and melanoma tissue. Scale bar, 50 μm. (c) Kaplan-Meier curves from patients with melanoma expressing low and high USP7 from the TCGA protein expression array data.

Fig. 2 Effects of USP7 on melanoma cell lines growth. (a,b) Protein lysates were extracted from A375 cells expressing transiently USP7 siRNA and stably control shRNA or USP7 shRNA   and B16 cells deleted the USP7 gene using the CRISPR/Cas9 editing system (USP7 KO). Western blotting analysis was performed to determine the expression of USP7. (b) Cells were collected from the indicated cells with gen6776 (USP7 inhibitor), USP7 shRNA or USP7 knocked out treatment. Colony formation assay was performed and represent images are shown. (c~e) A375 cells were transfected with USP7 siRNAs for 48h and detected with Annexin V- FITC/PI staining followed by flow cytometry analysis. Cell death populations were shown. Western blotting analysis was used for PARP expression.（f~h）A375 cells were treated as described in (c~e). Immunofluorescence staining of Ki-67 of A375 cells was observed using fluorescence microscope. Red: Ki-67; blue: nucleus. Typical image is shown. Scale bars: 50μm. And the analysis of cell cycle by FCM was described in the "Materials and methods". Data represent a mean ± SEM of three independent experiments, each in triplicate; bars, SEM. *P ≤ 0.05 vs. control.

Fig. 3 GO annotation and KEGG pathway analysis of the DEPs. (a) Top 10 enriched GO terms under "biological process". Term01, microtubule-based movement; term02, CTP metabolic process; term03, CTP biosynthetic process; term04, platelet degranulation; term05, pyrimidine ribonucleoside triphosphate biosynthetic process; term06, microtubule-based transport; term07, transport along microtubule; term08, pyrimidine ribonucleoside triphosphate metabolic process; term09, pyrimidine nucleoside triphosphate biosynthetic process; term10, pyrimidine ribonucleoside biosynthetic process.

Top 10 enriched GO terms under "molecular function". Term01, microtubule motor activity; term02, transition metal ion transmembrane transporter activity; term03, uridine kinase activity; term04, motor activity; term05, nucleobase-containing compound kinase activity; term06, alcohol binding; term07, clathrin heavy chain binding; term08, ferric iron binding; term09, zinc ion transmembrane transporter

qactivity; term10, divalent inorganic cation transmembrane transporter activity. (b) Protein–protein interaction network generated with STRING and visualized with Cytoscape for DEPs. DEPs are represented as round nodes. The red node indicates upregulation or green node indicates downregulation of the DEPs. Corresponding to proteins related to DNA repair (1), post-transiational protein modification and iron ion transport (2), microtubule motor activity (3), metal ion binding (4) and ubiquitin-protein transferase activity (5), ubiquitin-protein transferase activity(6). (c) Enriched KEGG pathways.

Fig. 4 Multiple proteins and PI3K/AKT/FOXO and AMPK signaling pathways are affected by removal of USP7. USP7 was inhibited by siRNA or inhibitor gen 6776 in A375 cells and was knocked out through CRISPR/Cas9 in B16 cells. (a) Proteins exhibiting significant changes between USP7 konckdown A375 cells and A375 cells and USP7-KO B16 cells. Protein names, USP7/NC ratio and the expression of indicated proteins by western blotting are shown. (b) The key proteins levels of PI3K/Akt/FOXO and AMPK siglaling pawthway were analyzed by western blotting after inactivation of USP7 in A375 cells and B16 cells. (c,d) The expressing of FOXO4 in nuclear and cytosol were detected by immunofluorescence and western blotting, respectively. Green, FOXO4; blue, nucleus. scale bar 50μm. (e) Representative the levels of P27^{kip1} by quantitative real-time PCR. Data represent a mean ± SEM of three independent experiments, each in triplicate; bars, SEM. **$P \leq 0.01$ vs. control.

Fig.5 USP7 function loss suppresses melanoma tumour growth *in vivo*.

Balb/c nude mice and C57BL mice were subcutaneously transplanted A375 cells stably expressing USP7 shRNA and USP7-KO B16 cells as indicated in the Materials and Methods, respectively. (a) The display images of harvested mice and tumors from A375 shRNA-NC cells, A375 shRNA-USP7 cells, B16 WT melonoma cells or B16 USP7-KO melonoma cells treatments respectively. (b) Mouse weight evolution during the experiment. The values are expressed as the mean. (c) Tumor size was determined by caliper measurement and the data were converted to tumor growth curves. (d) Tumor tissues were harvested, and weighed at the end of study (**, $P < 0.01$. Error bar =S.D.). (e and f) The expressions of indicated proteins in tumor tissues were measured by western blotting and immunohistochemistry.
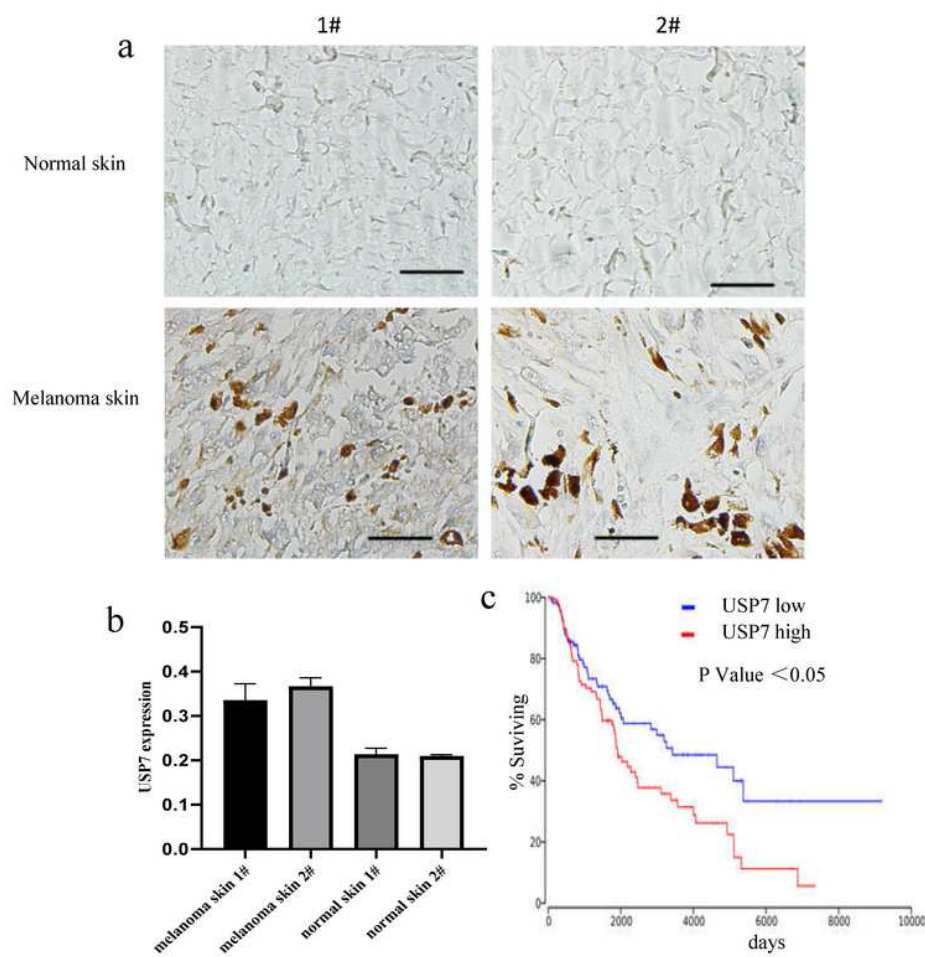
Figures

Figure 1

USP7 is overexpressed in melanoma and predicts clinical outcome. (a,b) Immunohistochemical analysis of USP7 in human normal skin and melanoma tissue. Scale bar, 50 μm. (c) Kaplan-Meier curves from patients with melanoma expressing low and high USP7 from the TCGA protein expression array data.
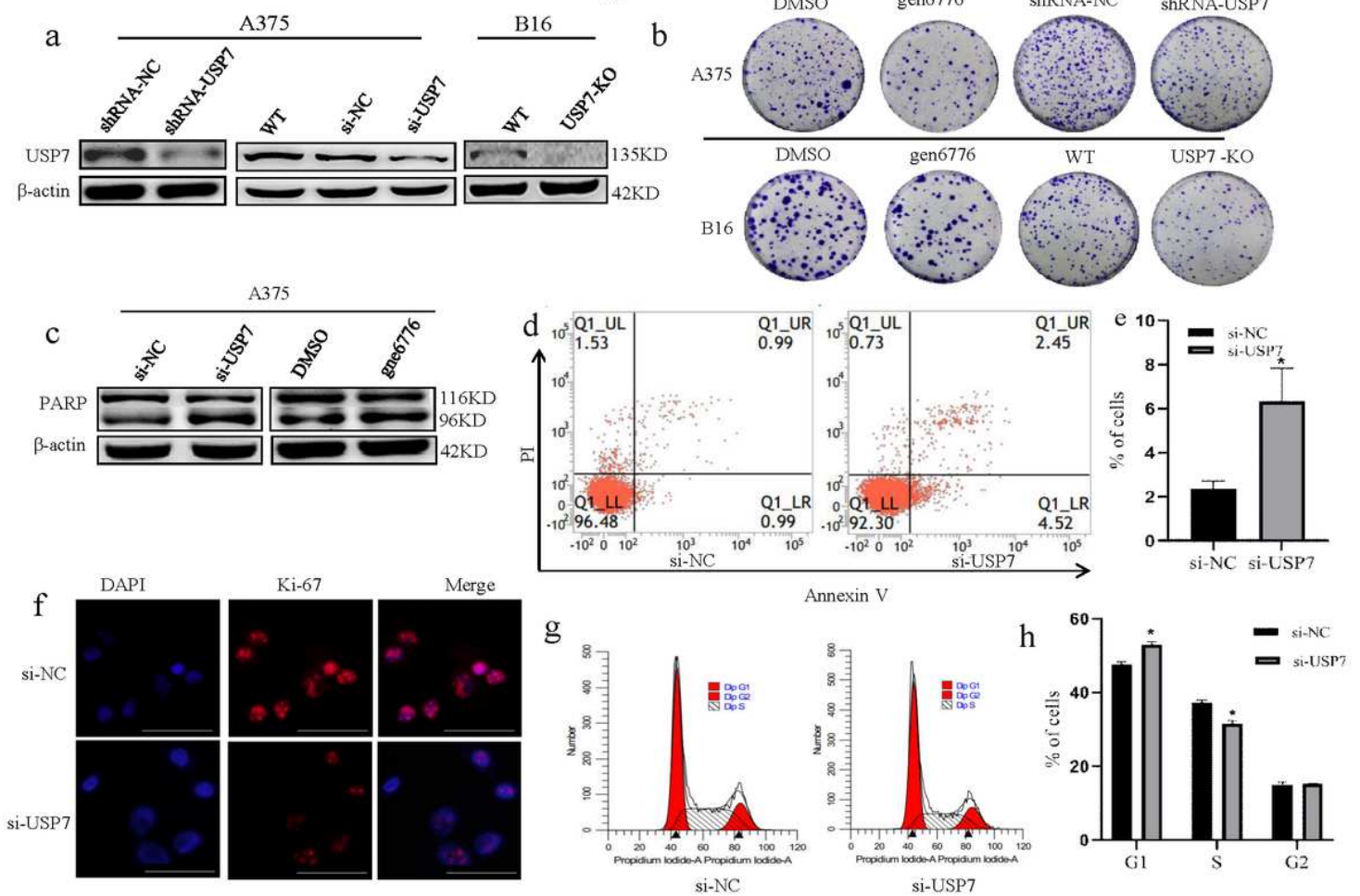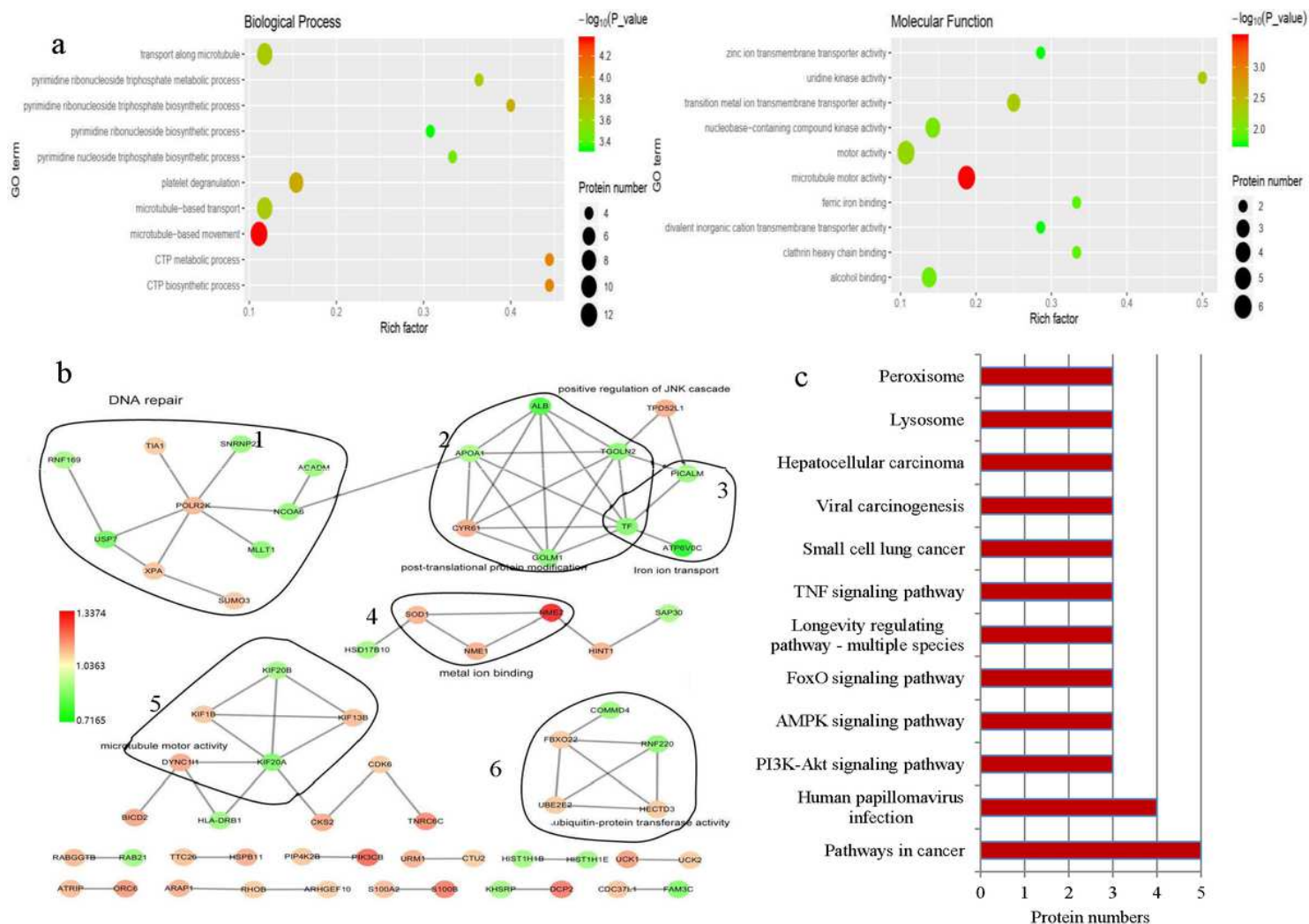
Figure 2

Effects of USP7 on melanoma cell lines growth. (a,b) Protein lysates were extracted from A375 cells expressing transiently USP7 siRNA and stably control shRNA or USP7 shRNA and B16 cells deleted the USP7 gene using the CRISPR/Cas9 editing system (USP7 KO). Western blotting analysis was performed to determine the expression of USP7. (b) Cells were collected from the indicated cells with gen6776 (USP7 inhibitor), USP7 shRNA or USP7 knocked out treatment. Colony formation assay was performed and represent images are shown. (c~e) A375 cells were transfected with USP7 siRNAs for 48h and detected with Annexin V- FITC/PI staining followed by flow cytometry analysis. Cell death populations were shown. Western blotting analysis was used for PARP expression.（f~h）A375 cells were treated as described in (c~e). Immunofluorescence staining of Ki-67 of A375 cells was observed using fluorescence microscope. Red: Ki-67; blue: nucleus. Typical image is shown. Scale bars: 50μm. And the analysis of cell cycle by FCM was described in the "Materials and methods". Data represent a mean ± SEM of three independent experiments, each in triplicate; bars, SEM. *P ≤ 0.05 vs. control

Figure 3

GO annotation and KEGG pathway analysis of the DEPs. (a) Top 10 enriched GO terms under "biological process". Term01, microtubule-based movement; term02, CTP metabolic process; term03, CTP biosynthetic process; term04, platelet degranulation; term05, pyrimidine ribonucleoside triphosphate biosynthetic process; term06, microtubule-based transport; term07, transport along microtubule; term08, pyrimidine ribonucleoside triphosphate metabolic process; term09, pyrimidine nucleoside triphosphate biosynthetic process; term10, pyrimidine ribonucleoside biosynthetic process. Top 10 enriched GO terms under "molecular function". Term01, microtubule motor activity; term02, transition metal ion transmembrane transporter activity; term03, uridine kinase activity; term04, motor activity; term05, nucleobase-containing compound kinase activity; term06, alcohol binding; term07, clathrin heavy chain binding; term08, ferric iron binding; term09, zinc ion transmembrane transporter qactivity; term10, divalent inorganic cation transmembrane transporter activity. (b) Protein−protein interaction network generated with STRING and visualized with Cytoscape for DEPs. DEPs are represented as round nodes. The red node indicates upregulation or green node indicates downregulation of the DEPs. Corresponding to proteins related to DNA repair (1), post-transiational protein modification and iron ion transport (2),

microtubule motor activity (3), metal ion binding (4) and ubiquitin-protein transferase activity (5), ubiquitin-protein transferase activity(6). (c) Enriched KEGG pathways.
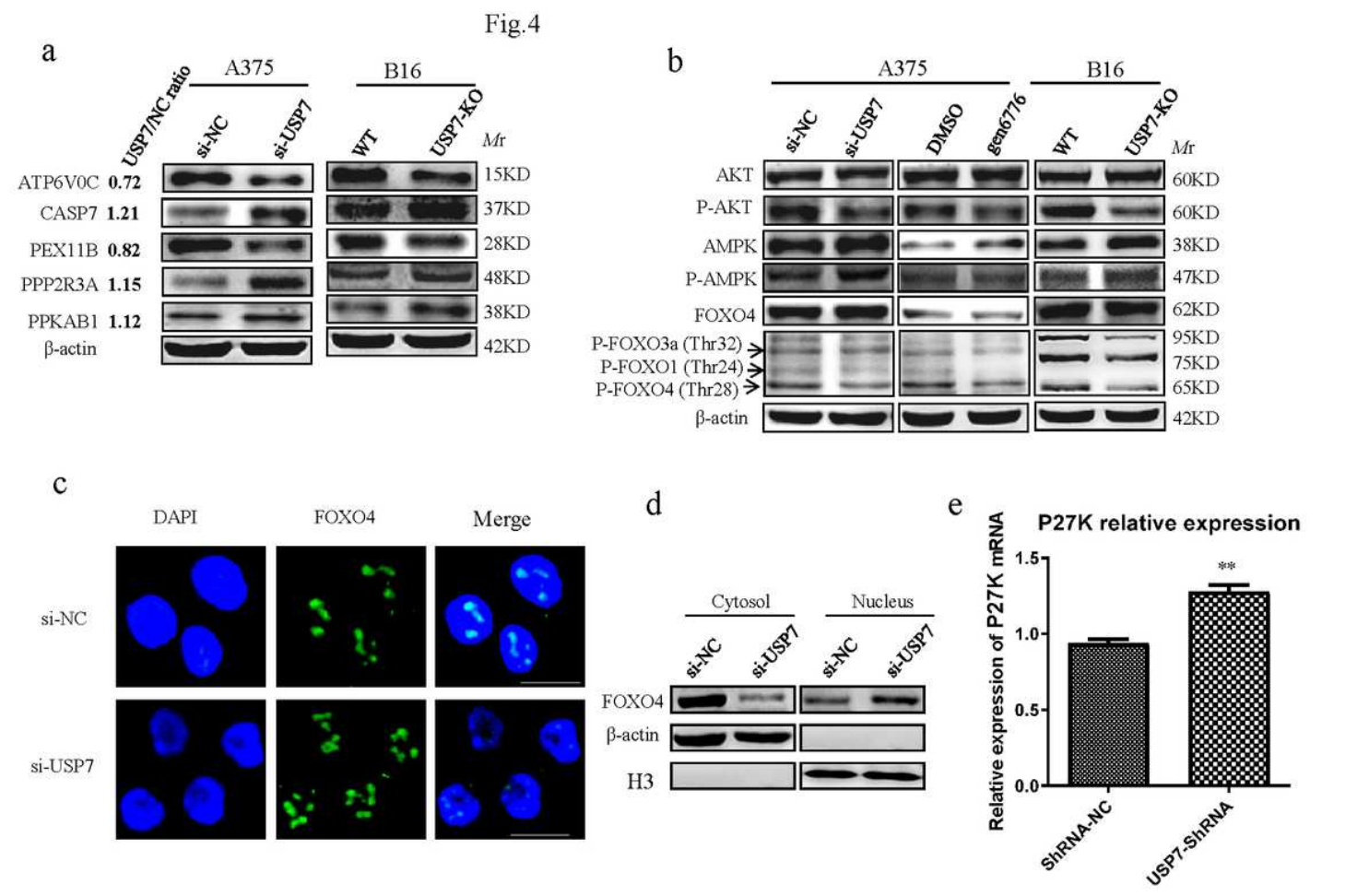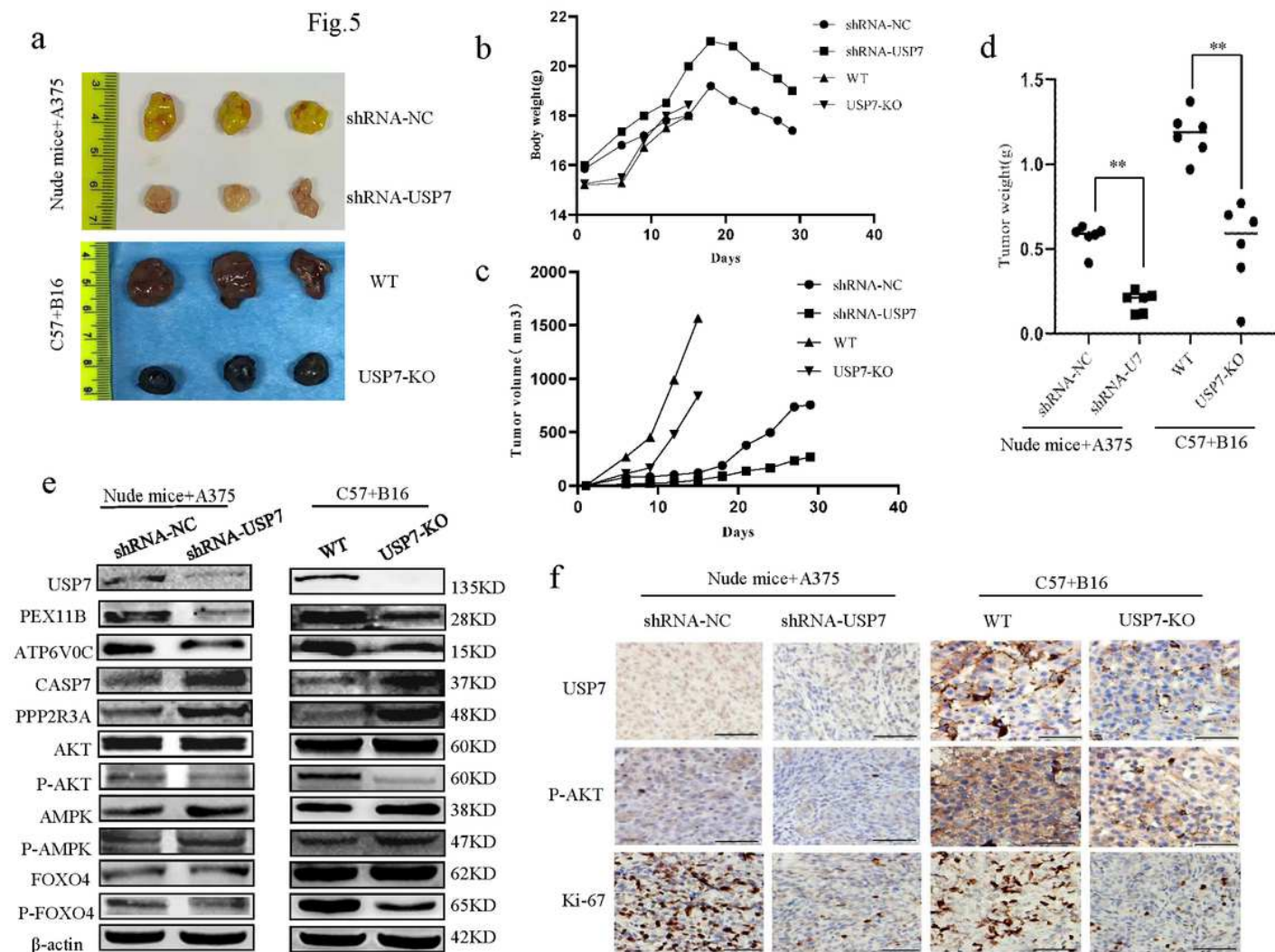

Figure 4

Multiple proteins and PI3K/AKT/FOXO and AMPK signaling pathways are affected by removal of USP7. USP7 was inhibited by siRNA or inhibitor gen 6776 in A375 cells and was knocked out through CRISPR/Cas9 in B16 cells. (a) Proteins exhibiting significant changes between USP7 konckdown A375 cells and A375 cells and USP7-KO B16 cells. Protein names, USP7/NC ratio and the expression of indicated proteins by western blotting are shown. (b) The key proteins levels of PI3K/Akt/FOXO and AMPK siglaling pawthway were analyzed by western blotting after inactivation of USP7 in A375 cells and B16 cells. (c,d) The expressing of FOXO4 in nuclear and cytosol were detected by immunofluorescence and western blotting, respectively. Green, FOXO4; blue, nucleus. scale bar 50μm. (e) Representative the levels of P27kip1 by quantitative real-time PCR. Data represent a mean ± SEM of three independent experiments, each in triplicate; bars, SEM. **$P \leq 0.01$ vs. control.

Figure 5

USP7 function loss suppresses melanoma tumour growth in vivo. Balb/c nude mice and C57BL mice were subcutaneously transplanted A375 cells stably expressing USP7 shRNA and USP7-KO B16 cells as indicated in the Materials and Methods, respectively. (a) The display images of harvested mice and tumors from A375 shRNA-NC cells, A375 shRNA-USP7 cells, B16 WT melonoma cells or B16 USP7-KO melonoma cells treatments respectively. (b) Mouse weight evolution during the experiment. The values are expressed as the mean. (c) Tumor size was determined by caliper measurement and the data were converted to tumor growth curves. (d) Tumor tissues were harvested, and weighed at the end of study (**, P < 0.01. Error bar =S.D.). (e and f) The expressions of indicated proteins in tumor tissues were measured by western blotting and immunohistochemistry.

Supplementary Files

This is a list of supplementary files associated with this preprint. Click to download.

- Suppplementary.pdf
- Table1.pdf
- Table1.pdf
- Suppplementary.pdf